Nanoporous Graphene Membranes for Organic Solvent Nanofiltration

Subjects: Engineering, Chemical

Contributor: Dae Woo Kim

The organic solvent nanofiltration (OSN) technique has attracted significant attention in separation processes in the chemical and pharmaceutical industries because it can serve as an integrated system, has high energy efficiency at mild operating conditions. Nanoporous graphene has been used for OSN membrane fabrication and ultrafast solvent permeance with precise molecular separation has been demonstrated.

Keywords: graphene ; nanopore ; organic solvent nanofiltration

1. Introduction

The organic solvent nanofiltration (OSN) technique has attracted significant attention in separation processes in the chemical and pharmaceutical industries because it can serve as an integrated system, has high energy efficiency, and exhibits minimal degradation at mild operating conditions [1][2]. In contrast to gas and water separation membranes, OSN membranes must be stable in harsh organic solvents with precise selectivity for small molecules in the nm or Å scales. Thus, graphitic materials such as graphene, graphene oxide (GO), reduced graphene oxide (rGO), and graphene oxide nanoribbons (GONRs) have been used for membrane fabrication because of their excellent chemical stability and mechanical properties, owing to the strong sp^2 hybridization of carbon atoms [3][4][5][6]. The one-atom-thick, two-dimensional (2D) shape of graphene with a high aspect ratio enables the deposition of an ultrathin selective layer on a porous support, resulting in a high solvent flux. Large-scale fabrication of graphene membranes can be done using continuous coating methods, such as slot-die coating and bar-coating [7][8][9][10]. In addition, molecular separation can be achieved by either a narrow interlayer spacing or nanopores on the basal plane.

Because of the aforementioned reasons, conceptual research on using graphene-based membranes for water treatment has been widely conducted, and a similar approach has been applied to OSN processes [11][12][13]. However, graphene layers are intrinsic barriers that also prevent the permeation of hydrogen and helium; therefore, the low permeation of organic solvents has been reported without any structural modification [14][15]. Thus, numerous approaches have been attempted to enhance the OSN performance by modifying the graphene structure. The application areas of the OSN process have been thoroughly discussed in previous studies; therefore, this review focuses on the current techniques used for tailoring the pore structure of the graphene layer and its effect on the OSN performance. Future perspectives of NG and current challenges faced are also discussed.

Recently, several graphene-based membranes that are used for water treatment or gas separation have been reported [16][17][18][19][20]. While single-layer nanoporous graphene (NG) membranes have been reported for their significantly thin selective layers, GO-based membranes have been reported, owing to their easy fabrication and precise molecular separation by narrow interlayer spacing. Compared to the research on water treatment membranes, the research on graphene-based OSN membranes is at an early stage. When only graphene is used for membrane fabrication, three approaches can be classified depending on their membrane structure: single-layer NG, multilayer graphene laminates, and multilayer NG laminates (**Figure 1**).

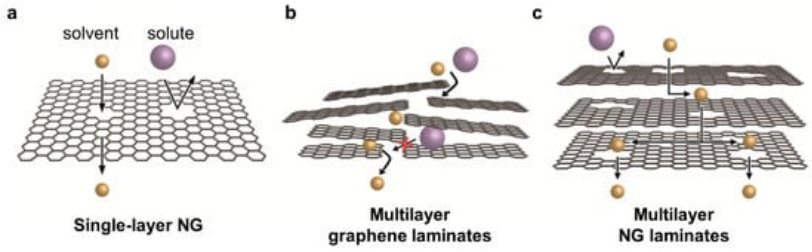

Figure 1. Three categories of graphene-based membrane used for OSN: (**a**) single-layer NG, (**b**) multilayer graphene laminates, and (**c**) multilayer NG laminates.

2. Methods for Introducing Nanopores in Graphene

Intrinsically, pristine single-layer graphene is a barrier that prevents the permeation of small molecules, including helium (He), hydrogen (H_2), and water. This is ascribed to the high electron density of its aromatic rings in the basal plane [14][15][21]. In addition, when GO is reduced to rGO, the effective interlayer spacing of rGO is negligible, and, thus, the small gas molecules do not penetrate the barrier [22]. The interlayer spacing of GO can be tuned by changing the type of organic solvent and the degree of swelling (**Figure 1**b); however, the molecules of the organic solvent are larger than those of water, and, thus, the permeation resistance to organic solvents can be much higher than to water. Therefore, a low or barrier-like organic solvent permeance was reported using a GO-based membrane, which can be beneficial for the dehydration of organic solvents [23][24].

Nanopore generation is a direct and effective method for enhancing the solvent permeance of graphene-based membranes. For single-layer graphene prepared by chemical vapor deposition (CVD) (**Figure 1**a), various top-down methods, such as focused ion beam, focused electron beam, ultraviolet-induced oxidative etching, ion bombardment followed by chemical etching, and oxygen plasma etching, have been used [25][26][27][28][29]. After transferring the CVD-grown graphene layer to a porous support, nanopores can be introduced by physical or chemical etching. For example, accelerated gallium ions generate defects on the plane, and further strong etching enlarges the pores (**Figure 2**a). As shown in **Figure 2**b,c, the formation of randomly distributed nanopores on the graphene layer can be confirmed by scanning transmission electron microscopy (STEM). By varying the exposure time in the chamber, the pore size and density of the nanopores can be tuned, as confirmed by the increased intensities of the D and D' peaks in the Raman spectra (**Figure 2**d,e). Because single-layer or few-layer graphene is used as the selective layer, the membrane thickness can be significantly decreased to the atomic scale. However, as such processes are performed under high-vacuum conditions and post-treated in a chamber, most studies are limited to a small-scale fabrication, while Yang et al. demonstrated its fabrication up to cm-scale [30].

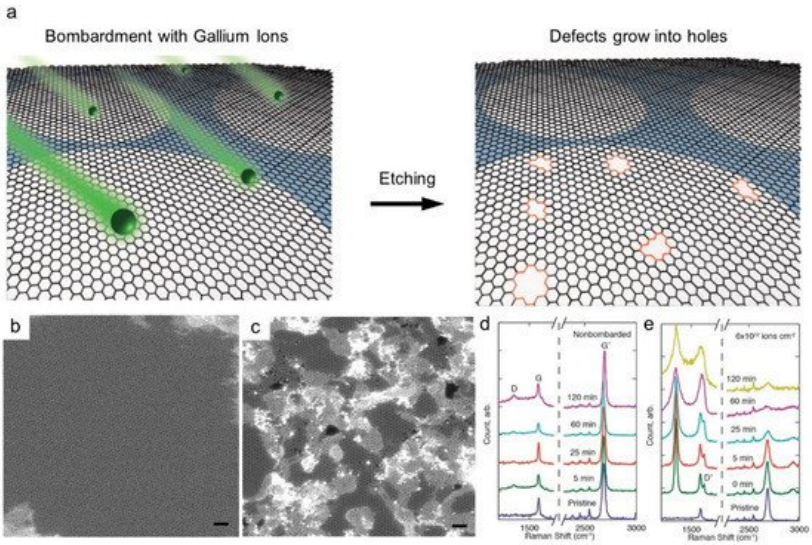

Figure 2. Membrane made of CVD-grown single layer graphene (**a**) Nanopore generation by ion bombardment followed by chemical oxidation. (**b**,**c**) TEM image of single layer graphene (**b**) and after (**c**) ion bombardment. Scale bars are 1 nm. (**d**,**e**) Raman spectra depending on chemical etching time and ion bombardment [25]. Copyright 2014 American Chemistry Society.

As an alternative method, the nanopores can be generated in GO on a large scale by post-treatment of GO powder; some examples of post-treatments are MnO_2 etching, KOH activation, H_2O_2 treatment, and rapid thermal treatment [31][32][33][34][35]. Intrinsic defects and holes are present in the original GO, formed during the synthesis of GO, but the size and density of the pores are negligible and not controlled. Because such post-treatments generate nanopores by the decomposition of oxygen-functional groups or defective sp^2 carbon on the GO plane, dense sp^3 carbon is formed near the pores, and oxygen-functional groups are also partially present. The defective structure is critical to tune the interlayer spacing to enable the permeation of large organic solvents through the nanochannel. Moreover, because NG is soluble in water and organic solvents, it is beneficial to fabricate laminated membranes by solution processes such as vacuum filtration, spin coating, bar coating, spray coating, and slot-die coating (**Figure 1**c). As observed by transmission electron microscopy (TEM), the size of most nanopores generated by post-treatment was in the range of several nm, while the sizes of the

sub-nm-sized micropores can be determined by gas adsorption. The pore size distribution of NG after post-treatment is typically broad; thus, the development of a more precise pore control method is required for the fabrication of highly selective membranes. On the other hand, the bottom-up synthesis of NG has also been attempted by surface-assisted aryl-aryl coupling reactions. However, membranes cannot be fabricated using synthesized graphene because the sheet is insufficient for deposition on a porous support. Thus, the achieved quality of exfoliation of graphene is unsatisfactory [36].

3. OSN Performance of NG-Based Membranes

The latest 2D material-based membranes and their OSN performance, including solvent permeation, solute rejection, and molecular weight cutoff (MWCO), are summarized in **Table 1**. The material types are categorized into transition metal carbides and nitrides (MXenes), transition metal dichalcogenides (TMDs), covalent organic frameworks (COFs), metal organic frameworks (MOFs), layered double hydroxides (LDHs), boron nitride, and NG-based membranes. All these membranes included a common thin-film composite-type membrane in which a selective graphene layer was fabricated on a porous support. Because the graphene layer is typically thin, on the nm scale, an additional freestanding porous support is essFiguretial for ensuring the mechanical stability of the membranes. Although the size and density of the porous support can affect the OSN performance, we focused on the material type of the selective layer, considering the optimized performance under each condition. As the viscosity of the solvent is inversely proportional to the permeance, the filtered solvents are also listed in the table. The details of the NG-based membrane are discussed below.

Table 1. Summary of the organic solvent nanofiltration performance of 2D material-based membranes.

Type	Material	Permeance (a)	Rejection (b)	MWCO (c)	Fabrication Method	Filtered Solvent	REF
MXene	Ti_3C_2Tx	982.7	AY79 (100%)	992	Vacuum filtration	Isopropanol	[37]
	PAN/PEI-$Ti_3C_2T_x$-NH_2	3	PEG800 (96%)	200	Drop casting	Isopropanol	[38]
	$Ti_3C_2T_x$/CNTs-CTAB	60.8	CR (>95%)	697	Vacuum filtration	Ethanol	[39]
TMD	S-MoS_2	636	MnB (99%) MB (100%)	320	Vacuum filtration	Isopropanol	[40]
	D-MoS_2	109	MnB (98%) BF (100%)	320	Vacuum filtration	Isopropanol	[40]
	WS_2-NMP-15	44.4	EB (99%) RBB (91.5%)	627	Pressure-assisted filtration	Ethanol	[41]
	(3PEI/5PSS-2.5MoS_2)$_{1.5}$	3.4	MnB (93.4%)	320	Layer by layer	Ethanol	[42]
COF	TAPA-TFP	127.3	BBR (94.8%)	826	Interfacial reaction	Ethanol	[43]
	GO/COF	50.8	MnB (99%) CR (99.8%)	320	Vacuum filtration	Ethanol	[44]
	SWCNT/COF	60.5	BBG (93%)	854	In-situ growth	Acetone	[45]
MOF	Zn-TCPP (Fe)	140	BBG (90%)	854	Vacuum filtration	Isopropanol	[46]
LDH	Mg-AlLDH	651	AF (99.6%) MO (98.3%)	327	Vacuum filtration	Acetone	[47]
	NiS_2/Ni-AlLDH	2464	MO (99.9%)	327	Vacuum filtration	Acetone	[48]
BN	FBN-2	330 †	CR (>99%)	697	Vacuum filtration	Ethanol	[49]
	FBN-8	240 †	MnB (93%)	320	Vacuum filtration	Methanol	[49]
Single-layer NG	Defect-sealed NG	170.7	RB (97.3%)	826	CVD	Methanol	[50]
		50.9	RB (95.9%)	826	CVD	Ethanol	[50]

Type	Material	Permeance [a]	Rejection [b]	MWCO [c]	Fabrication Method	Filtered Solvent	REF
Multilayer graphene	TPP/GO/HPEI	8.5	AB (95%)	1299	Pressure-assisted filtration	Ethanol	[51]
	PA/cGO/cross-linked PI	4.9	EY (100%) RhB (99.3%)	479	Immersion	Ethanol	[52]
	CW-GO	58.1	EB (96%)	248	Vacuum filtration	Methanol	[53]
	GO-Si2	290	RB (91.9%) CR (95.8%)	697	Vacuum filtration	Methanol	[54]
	GO-0.5BA-T	4	AF (95.8%)	586	Vacuum filtration	Methanol	[55]
	rGO-TMPyP$_{0.6}$-44	5.3	EB (>99.9%) AF (92.2%)	586	Vacuum filtration	Methanol	[56]
Multilayer NG	GO/EDA	0.5	VB (95.3%)	837	Pressure-assisted filtration	Isopropanol	[57]
	Shear-aligned GO	130	RhB (91%)	974	Gravure printing	Isopropanol	[58]
	Micro & nanosized GO	109.5	MnB (98%) FB (91%)	338	Vacuumfiltration	Isopropanol	[59]
	PI/GO	107.8	OII (96.3%) RB (99.9%)	350	Pressure-assisted filtration	Acetonitrile	[60]
	TNCS	1839	NBB (99%)	600	Vacuum filtration	Isopropanol	[32]
	NG-200	241	EB (99.9%) CR (98.9%)	616	Vacuum filtration	Isopropanol	[61]

AY79, Acid yellow 79; CR, Congo red; PEG, polyethylene glycol; MnB, methylene blue; MB, methyl blue; BF, basic fuchsin; EB, Evans blue; RBB, Remazol brilliant blue R; BBR, Brilliant blue R; BBG, Brilliant blue G; AF, Acid fuchsin; MO, Methyl orange; AB, Alcian blue 8GX; EY, eosin yellow; RhB, Rhodamine B; VB, Vitamin B12; FB, Fuchsin basic; OII, Orange II; NBB, naphtol blue black. PAN, polyacrylonitrile; PEI, polyethyleneimine; CTAB, Cetrimonium bromide; PSS, poly(sodium 4-styrenesulfonate; TAPA, tris(4-aminophenyl)amine; TFP, 2,4,6-triformylphloroglucinol; TCPP, tetra(4-carboxyphenyl)porphyrin; FBN, functionalized boron nitride; HPEI, hyperbranched polyethyleneimine; PI, polyimide; TNCS, turbostratic nanoporous carbon sheet. (a) Pure organic solvent permeance (L m^{-2} h^{-1} bar^{-1}). (b) Representative organic molecules used for the filtration test. (c) MWCO: Molecular weight at 90% rejection. † Dye permeance.

References

1. Marchetti, P.; Solomon, M.F.J.; Szekely, G.; Livingston, A.G. Molecular Separation with Organic Solvent Nanofiltration: A Critical Review. Chem. Rev. 2014, 114, 10735–10806.
2. Nie, L.A.; Chuah, C.Y.; Bae, T.H.; Lee, J.M. Graphene-Based Advanced Membrane Applications in Organic Solvent Na nofiltration. Adv. Funct. Mater. 2021, 31, 2006949.
3. Frank, O.; Tsoukleri, G.; Parthenios, J.; Papagelis, K.; Riaz, I.; Jalil, R.; Novoselov, K.S.; Galiotis, C. Compression Beha vior of Single-Layer Graphenes. ACS. Nano 2010, 4, 3131–3138.
4. Hod, O.; Scuseria, G.E. Electromechanical Properties of Suspended Graphene Nanoribbons. Nano Lett. 2009, 9, 2619 –2622.
5. Huang, L.; Zhang, M.; Li, C.; Shi, G.Q. Graphene-Based Membranes for Molecular Separation. J. Phys. Chem. Lett. 20 15, 6, 2806–2815.
6. Lee, C.; Wei, X.D.; Kysar, J.W.; Hone, J. Measurement of the Elastic Properties and Intrinsic Strength of Monolayer Gr aphene. Science 2008, 321, 385–388.
7. Akbari, A.; Sheath, P.; Martin, S.T.; Shinde, D.B.; Shaibani, M.; Banerjee, P.C.; Tkacz, R.; Bhattacharyya, D.; Majumder, M. Large-area Graphene-based Nanofiltration Membranes by Shear Alignment of Discotic Nematic Liquid Crystals of G raphene Oxide. Nat. Commun. 2016, 7, 10891.
8. Choi, Y.; Kim, S.S.; Kim, J.H.; Kang, J.; Choi, E.; Choi, S.E.; Kim, J.P.; Kwon, O.; Kim, D.W. Graphene Oxide Nanoribbo n Hydrogel: Viscoelastic Behavior and Use as a Molecular Separation Membrane. ACS Nano 2020, 14, 12195–12202.

9. Kim, J.H.; Choi, Y.; Kang, J.H.; Choi, E.; Choi, S.E.; Kwon, O.; Kim, D.W. Scalable Fabrication of Deoxygenated Graphene Oxide Nanofiltration Membrane by Continuous Slot-die Coating. J. Membr. Sci. 2020, 612, 118454.
10. Kwon, O.; Choi, Y.; Choi, E.; Kim, M.; Woo, Y.C.; Kim, D.W. Fabrication Techniques for Graphene Oxide-Based Molecular Separation Membranes: Towards Industrial Application. Nanomaterials 2021, 11, 757.
11. Joshi, R.K.; Carbone, P.; Wang, F.C.; Kravets, V.G.; Su, Y.; Grigorieva, I.V.; Wu, H.A.; Geim, A.K.; Nair, R.R. Precise and Ultrafast Molecular Sieving Through Graphene Oxide Membranes. Science 2014, 343, 752–754.
12. Morelos-Gomez, A.; Cruz-Silva, R.; Muramatsu, H.; Ortiz-Medina, J.; Araki, T.; Fukuyo, T.; Tejima, S.; Takeuchi, K.; Hayashi, T.; Terrones, M.; et al. Effective NaCl and Dye Rejection of Hybrid Graphene Oxide/Graphene Layered Membranes. Nat. Nanotechnol. 2017, 12, 1083–1088.
13. Yang, Q.; Su, Y.; Chi, C.; Cherian, C.T.; Huang, K.; Kravets, V.G.; Wang, F.C.; Zhang, J.C.; Pratt, A.; Grigorenko, A.N.; et al. Ultrathin Graphene-based Membrane with Precise Molecular Sieving and Ultrafast Solvent Permeation. Nat. Mater. 2017, 16, 1198–1202.
14. Bunch, J.S.; Verbridge, S.S.; Alden, J.S.; van der Zande, A.M.; Parpia, J.M.; Craighead, H.G.; McEuen, P.L. Impermeable Atomic Membranes from Graphene Sheets. Nano Lett. 2008, 8, 2458–2462.
15. Berry, V. Impermeability of Graphene and its Applications. Carbon 2013, 62, 1–10.
16. Abraham, J.; Vasu, K.S.; Williams, C.D.; Gopinadhan, K.; Su, Y.; Cherian, C.T.; Dix, J.; Prestat, E.; Haigh, S.J.; Grigorieva, I.V.; et al. Tunable Sieving of Ions using Graphene Oxide Membranes. Nat. Nanotechnol. 2017, 12, 546–550.
17. Chen, L.; Shi, G.S.; Shen, J.; Peng, B.Q.; Zhang, B.W.; Wang, Y.Z.; Bian, F.G.; Wang, J.J.; Li, D.Y.; Qian, Z.; et al. Ion Sieving in Graphene Oxide Membranes via Cationic Control of Interlayer Spacing. Nature 2017, 550, 415–418.
18. Kim, H.W.; Yoon, H.W.; Yoon, S.M.; Yoo, B.M.; Ahn, B.K.; Cho, Y.H.; Shin, H.J.; Yang, H.; Paik, U.; Kwon, S.; et al. Selective Gas Transport Through Few-Layered Graphene and Graphene Oxide Membranes. Science 2013, 342, 91–95.
19. Wang, L.; Williams, C.M.; Boutilier, M.S.H.; Kidambi, P.R.; Karnik, R. Single-Layer Graphene Membranes Withstand Ultrahigh Applied Pressure. Nano Lett. 2017, 17, 3081–3088.
20. Huang, S.Q.; Dakhchoune, M.; Luo, W.; Oveisi, E.; He, G.W.; Rezaei, M.; Zhao, J.; Alexander, D.T.L.; Zuttel, A.; Strano, M.S.; et al. Single-layer Graphene Membranes by Crack-free Transfer for Gas Mixture Separation. Nat. Commun. 2018, 9, 2632.
21. Sun, P.Z.; Yang, Q.; Kuang, W.J.; Stebunov, Y.V.; Xiong, W.Q.; Yu, J.; Nair, R.R.; Katsnelson, M.I.; Yuan, S.J.; Grigorieva, I.V.; et al. Limits on Gas Impermeability of Graphene. Nature 2020, 579, 229–232.
22. Su, Y.; Kravets, V.G.; Wong, S.L.; Waters, J.; Geim, A.K.; Nair, R.R. Impermeable Barrier Films and Protective Coatings based on Reduced Graphene Oxide. Nat. Commun. 2014, 5, 4843.
23. Liang, S.W.; Song, Y.M.; Zhang, Z.M.; Mu, B.W.; Li, R.; Li, Y.; Yang, H.; Wang, M.D.; Pan, F.S.; Jiang, Z.Y. Construction of Graphene Oxide Membrane through Non-covalent Cross-linking by Sulfonated Cyclodextrin for Ultra-permeable Butanol Dehydration. J. Membr. Sci. 2021, 621, 118938.
24. Shin, Y.; Taufique, M.F.N.; Devanathan, R.; Cutsforth, E.C.; Lee, J.; Liu, W.; Fifield, L.S.; Gotthold, D.W. Highly Selective Supported Graphene Oxide Membranes for Water-Ethanol Separation. Sci. Rep. 2019, 9, 2251.
25. O'Hern, S.C.; Boutilier, M.S.H.; Idrobo, J.C.; Song, Y.; Kong, J.; Laoui, T.; Atieh, M.; Karnik, R. Selective Ionic Transport through Tunable Subnanometer Pores in Single-Layer Graphene Membranes. Nano Lett. 2014, 14, 1234–1241.
26. Surwade, S.P.; Smirnov, S.N.; Vlassiouk, I.V.; Unocic, R.R.; Veith, G.M.; Dai, S.; Mahurin, S.M. Water Desalination using Nanoporous Single-layer Graphene. Nat. Nanotechnol. 2015, 10, 459–464.
27. Koenig, S.P.; Wang, L.D.; Pellegrino, J.; Bunch, J.S. Selective Molecular Sieving through Porous Graphene. Nat. Nanotechnol. 2012, 7, 728–732.
28. Fischbein, M.D.; Drndic, M. Electron Beam Nanosculpting of Suspended Graphene Sheets. Appl. Phys. Lett. 2008, 93, 113107.
29. Celebi, K.; Buchheim, J.; Wyss, R.M.; Droudian, A.; Gasser, P.; Shorubalko, I.; Kye, J.I.; Lee, C.; Park, H.G. Ultimate Permeation Across Atomically Thin Porous Graphene. Science 2014, 344, 289–292.
30. Yang, Y.B.; Yang, X.D.; Liang, L.; Gao, Y.Y.; Cheng, H.Y.; Li, X.M.; Zou, M.C.; Cao, A.Y.; Ma, R.Z.; Yuan, Q.; et al. Large-area Graphene-nanomesh/carbon-nanotube Hybrid Membranes for Ionic and Molecular Nanofiltration. Science 2019, 364, 1057–1062.
31. Kim, D.W.; Choi, J.; Kim, D.; Jung, H.T. Enhanced Water Permeation based on Nanoporous Multilayer Graphene Membranes: The Role of Pore Size and Density. J. Mater. Chem. A 2016, 4, 17773–17781.

32. Jang, J.; Nam, Y.T.; Kim, D.; Kim, Y.J.; Kim, D.W.; Jung, H.T. Turbostratic Nanoporous Carbon Sheet Membrane for Ultrafast and Selective Nanofiltration in Viscous Green Solvents. J. Mater. Chem. A 2020, 8, 8292–8299.

33. Xu, Y.X.; Lin, Z.Y.; Zhong, X.; Huang, X.Q.; Weiss, N.O.; Huang, Y.; Duan, X.F. Holey Graphene Frameworks for Highly Efficient Capacitive Energy Storage. Nat. Commun. 2014, 5, 4554.

34. Zhu, Y.W.; Murali, S.; Stoller, M.D.; Ganesh, K.J.; Cai, W.W.; Ferreira, P.J.; Pirkle, A.; Wallace, R.M.; Cychosz, K.A.; Thommes, M.; et al. Carbon-Based Supercapacitors Produced by Activation of Graphene. Science 2011, 332, 1537–1541.

35. Fan, Z.J.; Zhao, Q.K.; Li, T.Y.; Yan, J.; Ren, Y.M.; Feng, J.; Wei, T. Easy Synthesis of Porous Graphene Nanosheets and their use in Supercapacitors. Carbon 2012, 50, 1699–1703.

36. Bieri, M.; Blankenburg, S.; Kivala, M.; Pignedoli, C.A.; Ruffieux, P.; Mullen, K.; Fasel, R. Surface-Supported 2D Heterotriangulene Polymers. Chem. Commun. 2011, 47, 10239–10241.

37. Wang, J.T.; Chen, P.P.; Shi, B.B.; Guo, W.W.; Jaroniec, M.; Qiao, S.Z. A Regularly Channeled Lamellar Membrane for Unparalleled Water and Organics Permeation. Angew. Chem. Int. Ed. 2018, 57, 6814–6818.

38. Hao, L.; Zhang, H.Q.; Wu, X.L.; Zhang, J.K.; Wang, J.T.; Li, Y.F. Novel Thin-film Nanocomposite Membranes Filled with Multi-functional Ti3C2Tx Nanosheets for Task-specific Solvent Transport. Compos. Part A 2017, 100, 139–149.

39. Shao, D.D.; Zhang, Q.X.; Wang, L.; Wang, Z.Y.; Jing, Y.X.; Cao, X.L.; Zhang, F.; Sun, S.P. Enhancing Interfacial Adhesion of MXene Nanofiltration Membranes via Pillaring Carbon Nanotubes for Pressure and Solvent Stable Molecular Sieving. J. Membr. Sci. 2021, 623, 119033.

40. Ran, J.; Zhang, P.P.; Chu, C.Q.; Cui, P.; Ai, X.Y.; Pan, T.; Wu, Y.Y.; Xu, T.W. Ultrathin Lamellar MoS2 Membranes for Organic Solvent Nanofiltration. J. Membr. Sci. 2020, 602, 117963.

41. Tham, H.M.; Japip, S.; Chung, T.S. WS2 Deposition on Cross-linked Polyacrylonitrile with Synergistic Transformation to Yield Organic Solvent Nanofiltration Membranes. J. Membr. Sci. 2019, 588, 117219.

42. Jiang, S.D.; Koh, A.Y.K.; Chong, K.H.; Zhang, S. Opening Organic Solvent Pathways by Molybdenum Disulfide in Mixed Matrix Membranes for Molecular Separation. J. Membr. Sci. 2019, 585, 60–66.

43. Liu, J.T.; Han, G.; Zhao, D.L.; Lu, K.J.; Gao, J.; Chung, T.S. Self-standing and Flexible Covalent Organic Framework (COF) Membranes for Molecular Separation. Sci. Adv. 2020, 6, eabb1110.

44. Chen, L.; Wang, W.P.; Fang, Q.Y.; Zuo, K.C.; Hou, G.M.; Ai, Q.; Li, Q.L.; Ci, L.J.; Lou, J. High Performance Hierarchically Nanostructured Graphene Oxide/Covalent Organic Framework Hybrid Membranes for Stable Organic Solvent Nanofiltration. Appl. Mater. Today 2020, 20, 100791.

45. Manoranjan, N.; Zhang, F.; Wang, Z.Y.; Dong, Y.P.; Fang, W.X.; Zhang, Y.T.; Zhu, Y.Z.; Jin, J. A Single-Walled Carbon Nanotube/Covalent Organic Framework Nanocomposite Ultrathin Membrane with High Organic Solvent Resistance for Molecule Separation. ACS Appl. Mater. Interfaces 2020, 12, 53096–53103.

46. Lei, X.T.; Tay, S.W.; Ong, P.J.; Hong, L. Organic Dye Solution Nanofiltration by 2D Zn-TCPP(Fe) Membrane—Leverage of Chemical and Fluid Dynamic Effects. J. Ind. Eng. Chem. 2019, 78, 410–420.

47. Ang, E.H.; Velioglu, S.; Chew, J.W. Tunable Affinity Separation Enables Ultrafast Solvent Permeation through Layered Double Hydroxide Membranes. J. Membr. Sci. 2019, 591, 117318.

48. Ang, E.H.; Chew, J.W. Two-Dimensional Transition-Metal Dichalcogenide-Based Membrane for Ultrafast Solvent Permeation. Chem. Mater. 2019, 31, 10002–10007.

49. Chen, C.; Wang, J.M.; Liu, D.; Yang, C.; Liu, Y.C.; Ruoff, R.S.; Lei, W.W. Functionalized Boron Nitride Membranes with Ultrafast Solvent Transport Performance for Molecular Separation. Nat. Commun. 2018, 9, 1902.

50. Cheng, C.; Iyengar, S.A.; Karnik, R. Molecular Size-dependent Subcontinuum Solvent Permeation and Ultrafast Nanofiltration Across Nanoporous Graphene Membranes. Nat. Nanotechnol. 2021, 16, 989–995.

51. Hua, D.; Chung, T.S. Polyelectrolyte Functionalized Lamellar Graphene Oxide Membranes on Polypropylene Support for Organic Solvent Nanofiltration. Carbon 2017, 122, 604–613.

52. Li, Y.Y.; Li, C.; Li, S.X.; Su, B.W.; Han, L.H.; Mandal, B. Graphene Oxide (GO)-interlayered Thin-film Nanocomposite (TFN) Membranes with High Solvent Resistance for Organic Solvent Nanofiltration (OSN). J. Mater. Chem. A 2019, 7, 13315–13330.

53. Zhang, L.Y.; Zhang, M.C.; Liu, G.P.; Jin, W.Q.; Li, X.Y. Fungal Cell Wall-Graphene Oxide Microcomposite Membrane for Organic Solvent Nanofiltration. Adv. Funct. Mater. 2021, 31, 2100110.

54. Wang, S.F.; Mahalingam, D.; Sutisna, B.; Nunes, S.P. 2D-dual-spacing Channel Membranes for High Performance Organic Solvent Nanofiltration. J. Mater. Chem. A 2019, 7, 11673–11682.

55. Gao, T.T.; Wu, H.B.; Tao, L.; Qu, L.T.; Li, C. Enhanced Stability and Separation Efficiency of Graphene Oxide Membranes in Organic Solvent Nanofiltration. J. Mater. Chem. A 2018, 6, 19563–19569.
56. Gao, T.T.; Huang, L.; Li, C.; Xu, G.C.; Shi, G.Q. Graphene Membranes with Tuneable Nanochannels by Intercalating Self-Assembled Porphyrin Molecules for Organic Solvent Nanofiltration. Carbon 2017, 124, 263–270.
57. Li, B.F.; Cui, Y.; Japip, S.; Thong, Z.W.; Chung, T.S. Graphene Oxide (GO) Laminar Membranes for Concentrating Pharmaceuticals and Food Additives in Organic Solvents. Carbon 2018, 130, 503–514.
58. Akbari, A.; Meragawi, S.E.; Martin, S.T.; Corry, B.; Shamsaei, E.; Easton, C.D.; Bhattacharyya, D.; Majumder, M. Solvent Transport Behavior of Shear Aligned Graphene Oxide Membranes and Implications in Organic Solvent Nanofiltration. ACS Appl. Mater. Interfaces 2018, 10, 2067–2074.
59. Ai, X.Y.; Zhang, P.P.; Dou, Y.; Wu, Y.Y.; Pan, T.; Chu, C.Q.; Cui, P.; Ran, J. Graphene Oxide Membranes with Hierarchical Structures Used for Molecule Sieving. Sep. Purif. Technol. 2020, 230, 115879.
60. Liu, M.L.; Guo, J.L.; Japip, S.; Jia, T.Z.; Shao, D.D.; Zhang, S.; Li, W.J.; Wang, J.; Cao, X.L.; Sun, S.P. One-step Enhancement of Solvent Transport, Stability and Photocatalytic Properties of Graphene Oxide/polyimide Membranes with Multifunctional Cross-linkers. J. Mater. Chem. A 2019, 7, 3170–3178.
61. Kang, J.; Choi, Y.; Kim, J.P.; Kim, J.H.; Kim, J.Y.; Kwon, O.; Kim, D.I.; Kim, D.W. Thermally-induced Pore Size Tuning of Multilayer Nanoporous Graphene for Organic Solvent Nanofiltration. J. Membr. Sci. 2021, 637, 119620.